Characterization of lymphangiogenesis in a model of adult skin regeneration

Joseph M. Rutkowski, Kendrick C. Boardman and Melody A. Swartz

Characterization of lymphangiogenesis in a model of adult skin regeneration

Joseph M. Rutkowski,[1] Kendrick C. Boardman,[2] and Melody A. Swartz[1,2]

[1]*Institute of Bioengineering, École Polytechnique Fédérale de Lausanne, Lausanne, Switzerland;*
and [2]*Department of Biomedical Engineering, Northwestern University, Evanston, Illinois*

Rutkowski, Joseph M., Kendrick C. Boardman, and Melody A. Swartz. Characterization of lymphangiogenesis in a model of adult skin regeneration. *Am J Physiol Heart Circ Physiol* 291: H1402–H1410, 2006. First published April 28, 2006; doi:10.1152/ajpheart.00038.2006.—To date, adult lymphangiogenesis is not well understood. In this study we describe the evolution of lymphatic capillaries in regenerating skin and correlate lymphatic migration and organization with the expression of matrix metalloproteinases (MMPs), immune cells, the growth factors VEGF-A and VEGF-C, and the heparan sulfate proteogylcan perlecan, a key component of basement membrane. We show that while lymphatic endothelial cells (LECs) migrate and organize unidirectionally, in the direction of interstitial fluid flow, they do not sprout into the region but rather migrate as single cells that later join together into vessels. Furthermore, in a modified "shunted flow" version of the model, infiltrated LECs fail to organize into functional vessels, indicating that interstitial fluid flow is necessary for lymphatic organization. Perlecan expression on new lymphatic vessels was only observed after vessel organization was complete and also appeared first in the distal region, consistent with the directionality of lymphatic migration and organization. VEGF-C expression peaked at the initiation of lymphangiogenesis but was reduced to lower levels throughout organization and maturation. In mice lacking MMP-9, lymphatics regenerated normally, suggesting that MMP-9 is not required for lymphangiogenesis, at least in mouse skin. This study thus characterizes the process of adult lymphangiogenesis and differentiates it from sprouting blood angiogenesis, verifies its dependence on interstitial fluid flow for vessel organization, and correlates its temporal evolution with those of relevant environmental factors.

lymphatic; vasculogenesis; interstitial fluid flow; matrix metalloproteinase-9; perlecan

ADULT LYMPHANGIOGENESIS is an important process that occurs in wound healing and may play a role in lymphedema and cancer metastasis. Increasingly, the importance of lymphatic biology is being realized, and many key advances in the field have recently emerged, particularly in the identification and characterization of key molecular regulators of lymphangiogenesis (2, 28). Through the analysis of gene expression in embryonic development, for example, the control of the lymphatic endothelial cell (LEC) phenotype by Prospero-homeobox-1 (Prox 1) (42) and the requirement of neuropilin-2 (43) and podoplanin (31) expression by LECs in embryonic lymphatic vessel formation have been established. VEGF receptor-3 (VEGFR-3) (16) and its ligands VEGF-C (12, 14, 26) and VEGF-D (1) have been well established as critical for both embryonic and adult lymphangiogenesis, although VEGFR-3 ligation may not be required for lymphatic vessel maintenance (29). Developmental and mechanistic studies of these factors and others, including angiopoietin-1 (40) and -2 (7), are continuing to elucidate the molecular underpinnings of lymphangiogenesis.

Despite this emerging knowledge, lymphangiogenesis in adult tissues is not adequately understood. Regulators of developmental lymphangiogenesis may not necessarily have the same relevance in adult lymphangiogenesis or lymphatic regeneration, particularly considering that many of these factors play multiple roles in early development of both blood and lymphatic vessels before becoming specific to one type of endothelial cell in adulthood (28). Furthermore, many studies of adult lymphangiogenesis utilize models in which lymphatic growth is induced by orthotopic human tumor xenografts in mice (2) or by exogenous stimulation in alymphatic tissues (5, 20), which may not accurately reflect physiologically relevant situations.

We recently developed a mouse model of adult lymphangiogenesis in regenerating skin and used it to demonstrate the role of interstitial flow in lymphangiogenesis (4, 39). In this model, a small circumferential band of skin is removed from the middle of the tail, fitted with a gas-permeable silicone sleeve, and filled with collagen. The collagen provides a scaffold for tissue regeneration that is initially cell-free, allowing the infiltration of immune cells and ingrowth of blood and lymphatic vessels to be tracked both spatially and temporally as the tissue regenerates. Furthermore, the silicone sleeve keeps the wound moist and intact and prevents granulation; indeed, the regenerated skin is virtually identical to native skin except for the absence of hair follicles that do not regenerate. Importantly, the collagen scaffold serves as a fluid bridge for the one-way interstitial convection of lymph fluid between the distal and proximal halves of the tail. In other words, because lymph always flows from the tip of the mouse tail toward the body, interstitial fluid flow through the regenerating region will always be unidirectional.

We previously used this model to demonstrate that interstitial flow plays an organizational role in lymphangiogenesis, specifically showing that lymphatic capillaries develop in the direction of lymph flow. We had hypothesized that flow was necessary to create fluid channels in the regenerating region into which LECs migrate and organize into lymphatic vessels. This model was also used to demonstrate that although complete inhibition of lymphangiogenesis in regenerating skin could be achieved by systemic delivery of mF4-31C1, a VEGFR-3 blocking antibody (29), excess VEGF-C in the regenerating region could not enhance physiological lymphangiogenesis (9). This model has thus proven useful for studying the effects of established biochemical cues on lymphatic regeneration.

Address for reprint requests and other correspondence: M. A. Swartz, Laboratory for Mechanobiology and Morphogenesis, Institute of Bioengineering, École Polytechnique Fédérale de Lausanne, Station 15, 1015 Lausanne, Switzerland (e-mail: melody.swartz@epfl.ch).

Here we characterize the process of lymphangiogenesis in the regenerating skin model to assess relative timing, distribution, and importance of some potential key regulating factors relative to lymphatic growth. Specifically, we examine lymphatic growth and morphology at early (1, 3, 5, 7, and 10 days) and later (17, 25, and 60 days) time points in the regeneration process and correlate temporally the presence of VEGF-C, VEGF-A, the heparan sulfate proteoglycan (HSPG) perlecan (a key component of basement membrane), matrix metalloproteinases (MMPs), and immune cells to lymphatic growth and morphology. We demonstrate that lymphatic regeneration occurs via single LECs migrating with interstitial fluid flow and, later, after populating the region, coalescing into vessels. We also provide further evidence that interstitial fluid flow is necessary for LEC organization using a shunted flow modification of our model. We show that VEGF-C expression is decreased as the lymphatic vessels become connected and functional, at which time a discontinuous perlecan expression pattern begins to become present on the lymphatics. Also, our data suggest that MMP-9 may not be important in adult dermal lymphangiogenesis and support previous observations that macrophages may play a critical role (20).

MATERIALS AND METHODS

Animal and sample preparation. All studies utilized 6–8 wk old female BALB/c mice (Charles River); 3–5 mice were used at each time point. Mice were anesthetized with an intraperitoneal injection of ketamine (65 mg/kg), xylazine (13 mg/kg), and acepromazine (2 mg/kg). An analgesic, butorphanol (0.05 mg/kg), was administered subcutaneously twice daily for three days after the procedure. All protocols were approved by the Veterinary Authorities of the Canton Vaud according to Swiss law (protocol no. 1687).

Mice were prepared as described previously (4). Briefly, a 2-mm-wide circumferential band of dermal tissue was excised midway up the tail. The area was then covered with a gas-permeable silicone sleeve and filled with type I rat-tail collagen (BD Pharmingen, San Jose, CA). The sleeve was secured with Nexaband adhesive (Abbott, Abbott Park, IL) at the proximal edge. Mice were euthanized at specified times from 1–60 days after the procedure. Additionally, to test the hypothesis that interstitial fluid flow is necessary for lymphatic organization, a modified "shunted flow" model was prepared in three mice. In this modified model, a 2-mm-square excision was made instead of a circumferential excision, allowing for lymph to circumvent around the regenerating region through existing lymphatics in the intact tissue (Fig. 1).

After the animals were euthanized, a section of tail 8 mm long (containing the regenerating region along with some native distal and proximal tissue) was removed and flash frozen in liquid N_2. Tissue samples were transversely cryosectioned into 12- and 60-μm-thick sections and stored at −80°C until immunostaining.

To further examine the role of MMP-9 in this model, MMP-9-deficient mice on an FVB/NJ background, along with wild-type controls, were obtained (FVB.Cg-*Mmp9^{tm1Tvu}*/J; Jackson, Bar Harbor, ME). Nine female mice at 6 wk of age from the MMP-9-deficient strain and nine female FVB/NJ controls were prepared as described. Three mice from each group were euthanized at 17, 25, and 60 days.

Microlymphangiography. Mice were anesthetized as above, and the regeneration of the lymphatic vasculature was examined by fluorescence microlymphangiography (4, 38). A fluorescently labeled macromolecule (2,000-kDa fluorescein-conjugated dextran, 2 mg/ml; Molecular Probes, Carlsbad, CA) was injected intradermally at a constant pressure of 45 cm of water into the tip of the tail. As the fluorescent tracer was picked up and transported by the lymphatic vessels, it was clearly visible within dermal lymphatic capillaries, thus providing a
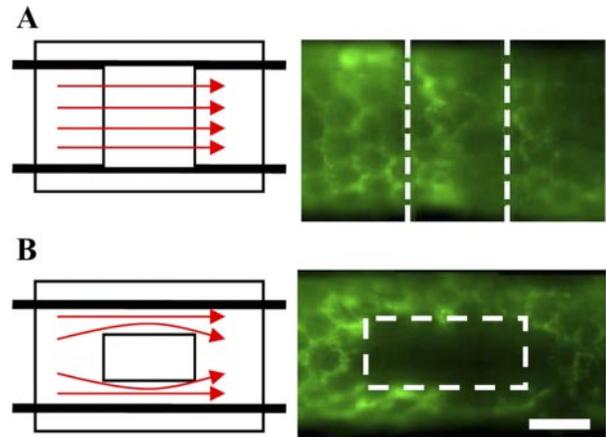

Fig. 1. Interstitial flow and mouse tail model of skin regeneration. *A*: in circumferential model, lymph flow from distal lymphatics (that is traveling in the proximal direction) must move interstitially through collagen implant to continue its flow in proximal lymphatic capillaries. Functional and organized lymphatic capillaries are seen by microlymphangiography at *day 60*. *B*: in square model, lymph flow is circumvented around implant in preexisting lymphatic capillaries, and entire lymphatic circuit is uninterrupted. Lymph does not become interstitial fluid in implant as in circumferential model, and thus interstitial flow through square implant is much less than that through circumferential implant. In shunted flow model, lymphatic endothelial cells (LECs) do not organize into a functional network (as evidenced by microlymphangiography), despite otherwise normal skin regeneration. In all microlymphangiography images, green indicates lymph fluid tracer (fluorescein-dextran) and thus identifies functional lymphatics and interstitial flow of postlymph through regenerating regions. Bar = 1 mm.

clear visualization of lymphatic functionality. The lymphatic vasculature was monitored with a Zeiss Axiovert 200M fluorescence microscope and Zeiss MRm camera.

Immunofluorescence and immunohistochemistry. To visualize blood endothelial cells (BECs) and LECs, both thin (12 μm) and thick (60 μm) sections were costained with primary antibodies to the lymphatic vessel endothelial hyaluronan receptor (LYVE-1; 1:500; rabbit polyclonal; Upstate, Charlottesville, VA) and endothelial cell marker CD31 (1:200; rat polyclonal; BD Pharmingen). Although CD31 has an affinity for lymphatics, costaining eliminated any discrepancy in identifying BECs from LECs. For immune cells and MMPs, thin (12 μm) sections were labeled using the following anti-mouse antibodies: the leukocyte-common CD45 (1:100; rat monoclonal; BD Pharmingen), the macrophage-specific surface marker F4/80 (1:50; rat monoclonal; Serotec, Raleigh, NC), the Langerhans dendritic cell protein langerin (1:50; goat polyclonal; Santa Cruz Biotechnology, Santa Cruz, CA), MMP-2 (1:25; goat polyclonal; R&D Systems, Minneapolis, MN), MMP-8 (1:100; goat polyclonal; Santa Cruz Biotechnology), MMP-9 (1:400; rabbit polyclonal; Chemicon, Temecula, CA), or MMP-13 (1:500; goat polyclonal; Chemicon). The heparan sulfate proteoglycan perlecan was also stained (1:500; rat monoclonal; US Biological, Swampscott, MA) together with LYVE-1. These antibodies were detected with Alexafluor 488 or 594-conjugated donkey, rabbit, and goat IgG secondary antibodies (1:200, Molecular Probes), counterstained with 4′,6-diamidino-2-phenylindole dihydrochloride (DAPI; Vector, Burlingame, CA). Thin sections were observed and imaged under a Zeiss Axiovert 200M fluorescence microscope with an Axiocam MRm camera. Confocal stacks of thick (60 μm) sections were scanned with the use of a Zeiss LSM 510 Meta confocal microscope, and maximum projections were generated for presentation.

VEGF-A and VEGF-C were labeled immunohistochemically. Sections were first fixed in 4% paraformaldehyde, blocked against endogenous biotin and avidin (Biotin Blocking System, Dako, Carpenteria, CA), and then labeled with VEGF-A (1:50; rabbit polyclonal;

Santa Cruz) or VEGF-C (1:50; goat polyclonal; Santa Cruz) and biotinylated secondary antibodies (1:200; AffiniPure donkey and rabbit, respectively; Jackson ImmunoResearch, West Grove, PA). These were then visualized using the ABC-AP kit and Vector Red (Vector). Sections were counterstained with hematoxylin, dehydrated, and mounted with Eukitt (Fluka Chemie AG, Buchs, Switzerland). Images were captured with an Olympus AX70 microscope and DP70 camera.

Image analysis. Images of the regenerating region were assembled into complete montages in Photoshop (Adobe Systems, San Jose, CA). LECs were defined as cells with a blue (DAPI-stained) nuclei surrounded by green (LYVE-1 with AlexaFluor 488) labeling. After the borders of the region were defined, the number of LECs within each half of the regenerating region was counted and summed across three random 12-μm sections from each animal. Similarly, Langerhans dendritic cells were counted by identifying nuclei of langerin-labeled cells in the regenerating regions of three 12-μm sections at each time point.

Metamorph 6.3 image analysis software (Molecular Devices, Sunnyvale, CA) was used for quantifying MMPs, growth factors, and other immune cells. For immune cells and MMPs, three regenerating region montages from like groups of images were analyzed to identify positive fluorescent labeling using intensity thresholding. The region was then clearly identified with a freehand tool (with care taken to exclude pockets or defects in the tissue sections), and the percentage of stained area within each regenerating region was obtained. Values for three regions were averaged. For growth factor quantification, the color range of Vector Red (Vector) staining, indicating positive labeling of either VEGF-A or VEGF-C, was identified, and the percent coverage of each regenerating region was similarly measured. The data were normalized for each factor to the maximum expression.

Statistics. ANOVA and two-tailed *t*-tests were performed to determine statistical significance. Data are reported as means $\pm$ SD. For MMPs, immune cells, and growth factors, the total expression during regeneration was compared with that of normal (control) tissue to determine significance in upregulation during regeneration. Additionally, a single-factor ANOVA was performed on expression during regeneration to determine whether there were significant differences among all of the time points.

RESULTS AND DISCUSSION

Unidirectional regeneration with interstitial fluid flow. First, we confirmed our earlier findings (4) that in regenerating mouse tail skin, lymphangiogenesis occurred in the direction of lymphatic flow (distal to proximal), which was also the direction of interstitial flow in the regenerating skin where lymph flow was interrupted. We further quantified this directionality in migration to demonstrate statistical significance (Fig. 2*F*). This was in contrast to blood angiogenesis, which occurred from all directions in the regenerating skin. Quantification of LECs in 12-μm sections revealed that the regenerating region was initially free of LECs and remained so through *day 10* (Fig. 2*E*). Although very few LECs were seen in the region at *day 10* (Fig. 2*B*), those present were confined to the distal half ($P = 0.007$) (Fig. 2*F*). At *day 17* (Fig. 2*C*), some LECs were present in the proximal half, but the distal population was much greater ($P < 0.001$). Even at later time points of 25 and 40 days, LECs populated the upstream (distal) region significantly more than the downstream region ($P = 0.04$ and $P = 0.006$ for 25 and 40 days, respectively), indicating that proliferation and migration were occurring primarily from the distal region. Even though the total number of LECs in the region did not significantly change after *day 17* (Fig. 2*E*), it was not until *day 60* (Fig. 2*D*), when functional and continuous lym-

phatic capillaries appeared normal, that the distribution of LECs was uniform throughout the regenerating region ($P = 0.4$ comparing distal vs. proximal).

To further explore whether interstitial flow is necessary for lymphatic organization, mice were prepared with a square regenerating region (as opposed to the circumferential model), which allows lymph flow to be circumvented around the implanted collagen gel in the intact lymphatic vessels. Unlike the circumferential collagen implant, where distal lymph must flow interstitially through the regenerating region to be picked up by functional lymphatics on the proximal side, lymph need not flow through the high-resistance regeneration zone in the square model because the intact surrounding lymphatic vessels provide a lower resistance to flow. Although this relative lack of directional interstitial flow did not inhibit reepithelialization or blood angiogenesis, we found that LECs failed to organize into a connected, functional lymphatic network in this shunted flow region (Fig. 1), demonstrating that interstitial fluid flow is necessary for functional lymphatic capillary organization.

Conversely, blood vessel regeneration was independent of the interstitial flow direction. Blood vessels initially appeared to sprout from the deeper, larger blood vessels underneath the regenerating region (near the bone) at *day 7*, and at *day 10*, sprouts were seen equally from distal and proximal edges as well (Fig. 2*B*). By *day 17*, blood vessels were present throughout the region. In the square shunted flow model, blood vessel regeneration was indistinguishable from that seen in the circumferential model (data not shown), as was reepithelialization of the collagen gel.

Lymphatic morphogenesis: coalescing rather than sprouting. Confocal microscopy of 60-μm sections revealed that in contrast to sprouting, LECs migrated as single cells (sometimes coalescing into small groups of cells) in the direction of interstitial flow and, after sufficiently populating the region, later organized into vessels. LECs were generally absent from the regenerating region until *day 10* when individual LECs or small groups were seen migrating into the distal half of the region (Fig. 3*A*). By *day 17*, multicellular groups or ducts were present (Fig. 3*B*) but were not connected to other groups. LECs predominantly began to organize in a fashion reminiscent of vasculogenesis by *day 25*. At this time, LECs in both the distal and proximal halves were already organized into vessel structures (Fig. 3*C*). At *day 60* (Fig. 3*D*) the regenerated region had a complete lymphatic vasculature, the morphology of which appeared similar to that of native vessels (Fig. 3*E*). In contrast, during concurrent blood angiogenesis, new blood vessels sprout directly from the existing native vasculature. Thus, by migrating as single cells in the direction of interstitial flow and then later coalescing into individual short vessel fragments and eventually into an interconnected capillary network, LEC organization into vessels was more reminiscent of vasculogenesis than of sprouting angiogenesis.

Development of basement membrane after lymphatic organization. Past analysis of endothelial cell basement membrane composition has shown that the predominant HSPG in the basement membrane of mature blood vessels is perlecan (33). This HSPG, produced in varying degrees by all endothelial cells (41), is essential for developmental vasculogenesis in mice (13) and is expressed during angiogenesis (34) and after vessel injury (15). Although lymphatic capillaries have a discontinuous basement membrane (37), it is not known at what
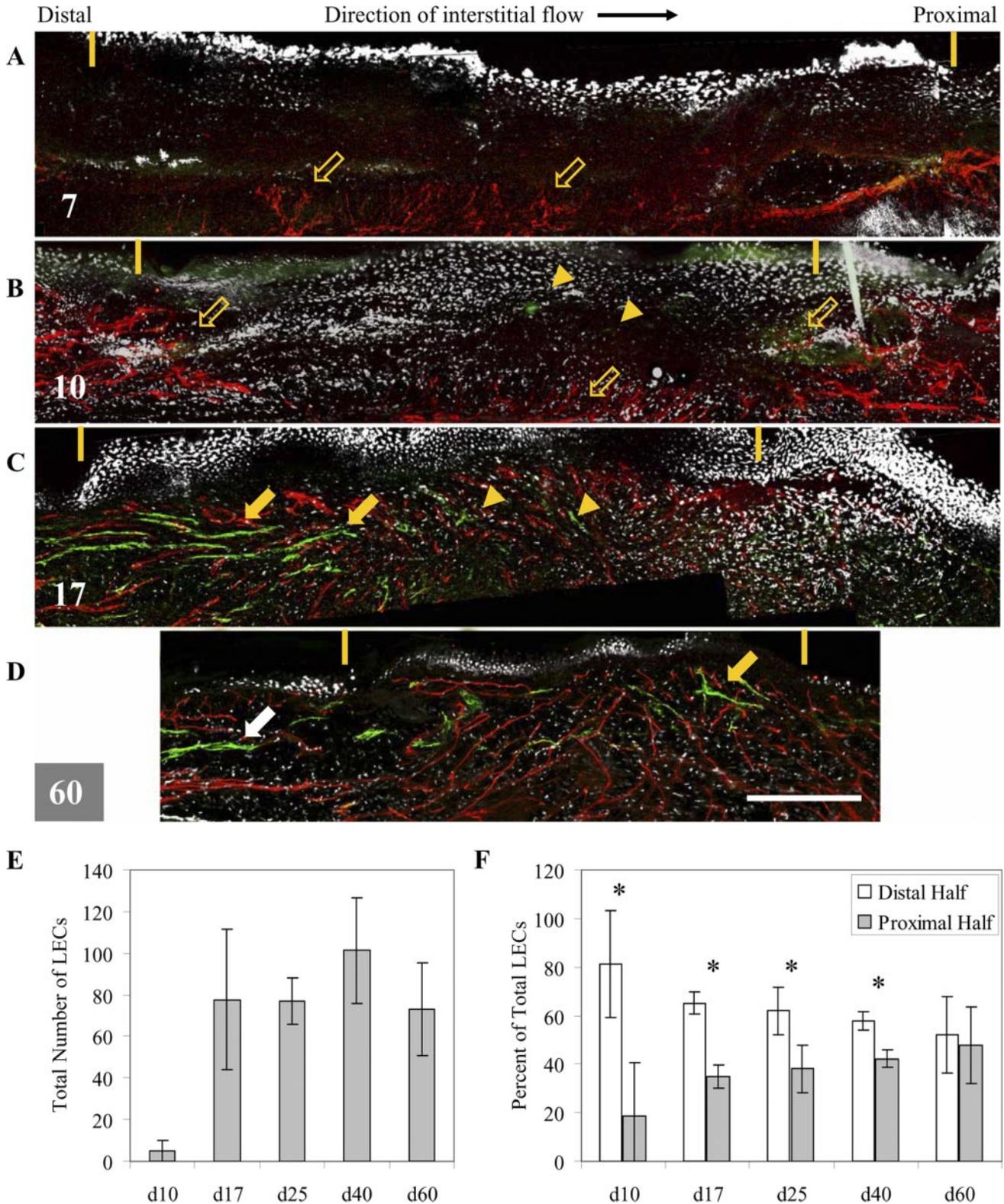
Fig. 2. Lymphatic regeneration occurs in direction of interstitial flow as shown by maximum projections of confocal scans. *A*: at 7 days, regenerating region (marked by yellow dashes) is free of LECs, but blood vessels (red) appear to sprout from deeper vessels (open arrows). *B*: at *day 10* (or d10), very few LECs (green marked by arrowheads) are seen, whereas blood vessel sprouting is present in all directions. *C*: at *day 17* (or d17), LECs (green) are seen in higher numbers in distal end of regenerating region, and more organization (arrows) is also seen in distal end. LECs in proximal half mostly remain as single cells. Blood vessels are present throughout regenerating region. *D*: at *day 60* (or d60), LECs are present throughout regenerating region and organized into an interconnected network, similar to that seen in native skin (white arrow). Note the overall contraction of regenerating region over time. Bar = 300 μm. *E*: quantification of total LECs in regenerating region confirms that LEC infiltration begins around *day 10*, is drastically increased at *day 17*, and is mostly complete by *day 25* (or d25). *F*: relative distribution of LECs in distal vs. proximal halves of regenerating region verifies qualitative observations that migration is primarily occurring from distal end. Through *day 40* (or d40), relative number of LECs in distal half is consistently and significantly greater than that in proximal half. By *day 60*, LEC distribution is normalized. *$P < 0.05$.

stage during lymphangiogenesis it develops. Using confocal microscopy on 60-μm sections, we observed perlecan colocalization with lymphatic vessels in regenerating skin only after organization had occurred, at *day 25* and *day 60* (Fig. 3).

Furthermore, its expression followed the spatial pattern of vessel formation and organization. At early times, before vessel organization was seen (*day 10* and *day 17*), perlecan expression was limited to new blood vessels. At *day 25* (Fig.
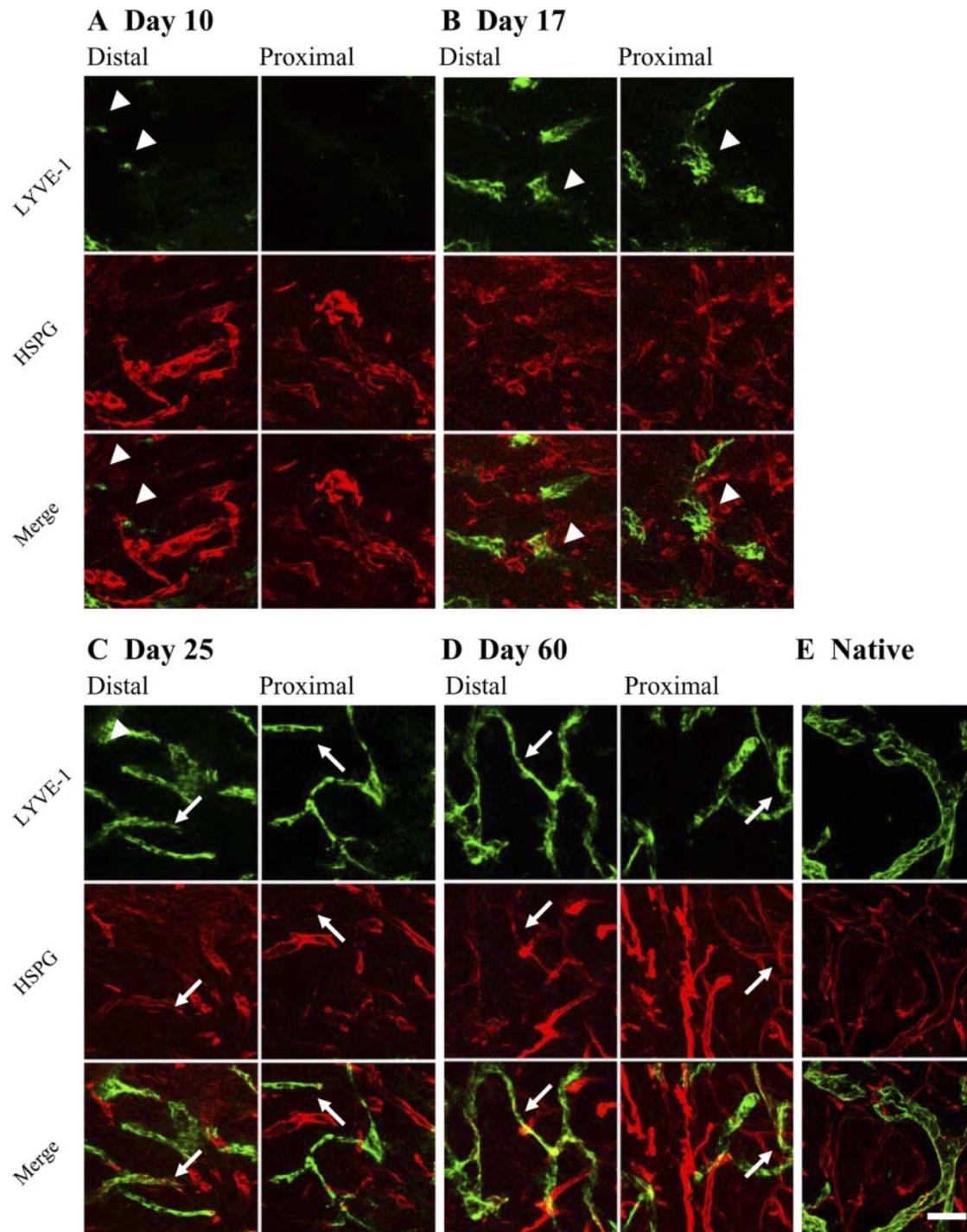

Fig. 3. Lymphangiogenesis as a process of cell migration and subsequent organization, rather than sprouting, with basement membrane developing after vessels become functional. Maximum projections of confocal scans are shown. *A*: at *day 10*, regenerating region is mostly free of LECs (green) with only a few LECs (arrowheads) present near distal end. Basement membrane proteoglycan perlecan (red) is readily detected on blood vessels. *B*: at *day 17*, LECs are present throughout entire regenerating region and organized into discrete and separate multicellular structures. Perlecan expression is not seen to be colocalized with any of these structures, indicating that basement membrane is absent in these primitive structures. *C*: at *day 25*, lymphatic organization is extensive and nearly complete. Perlecan is detected only on lymphatic vessels in distal half of regenerating region (arrows). *D*: by *day 60*, discontinuous perlecan staining pattern is present on nearly all lymphatic vessels (arrows), although staining is visibly stronger in distal half. *E*: lymphatic capillaries in native skin show strong perlecan staining. LYVE-1, lymphatic vessel endothelial hyaluronan receptor; HSPG, heparan sulfate proteoglycan. Bar = 50 μm.

3C), when significant organization of LECs into vessels was underway, some lymphatic structures in the distal half were perlecan positive, whereas those in the proximal half were not. By *day 60* (Fig. 3D), nearly all lymphatic vessels in the distal half were colocalized with perlecan, but in the proximal half where some vessels were still forming, perlecan expression appeared more sporadically. In normal intact skin, the lymphatic capillaries strongly expressed perlecan (Fig. 3E). Thus, because the HSPG perlecan identifies basement membrane on regenerating lymphatic vessels and appears only after vessel organization has occurred, it may be indicative of lymphatic vessel maturation. Additionally, its initial appearance only on distal vessels further demonstrates the directionality of both LEC migration and lymphatic organization in this model.

Early VEGF-A and VEGF-C upregulation. Expression of VEGF-A and VEGF-C was highest during the initiation of both blood and lymph angiogenesis. VEGF-A expression (Fig. 4) appeared to be highest at *day 5*, slightly preceding observable blood angiogenesis. These differences in expression, however,

were not statistically significant. VEGF-C expression (Fig. 4) was highest before, and during the initiation of, lymphangiogenesis (*days 3–10*). This expression was significantly higher at *days 3–10* than at *days 17* and *25* ($P = 0.033$). These expression profiles suggest that heightened expression of both VEGF-A and VEGF-C signaling might be most important in early (i.e., initiation) rather than later (i.e., organization and maturation) stages of vasculogenesis and lymphangiogenesis, consistent with their known functional roles (6, 28).

MMP expression. MMPs known to be upregulated in murine wound healing, specifically MMP-2, -8, -9, and -13 (3, 18, 19), were examined to determine their transient relationship to lymphatic regeneration. Our results suggest that only MMP-9 and -13 were significantly elevated in the regenerating region compared with normal control skin ($P = 0.006$ and 0.001, respectively), although the expression of MMP-2 was almost significantly higher during regeneration than in control tissue ($P = 0.056$) and appeared to peak at *day 17* (Fig. 4). MMP-2 and -9 play important roles in extracellular matrix remodeling
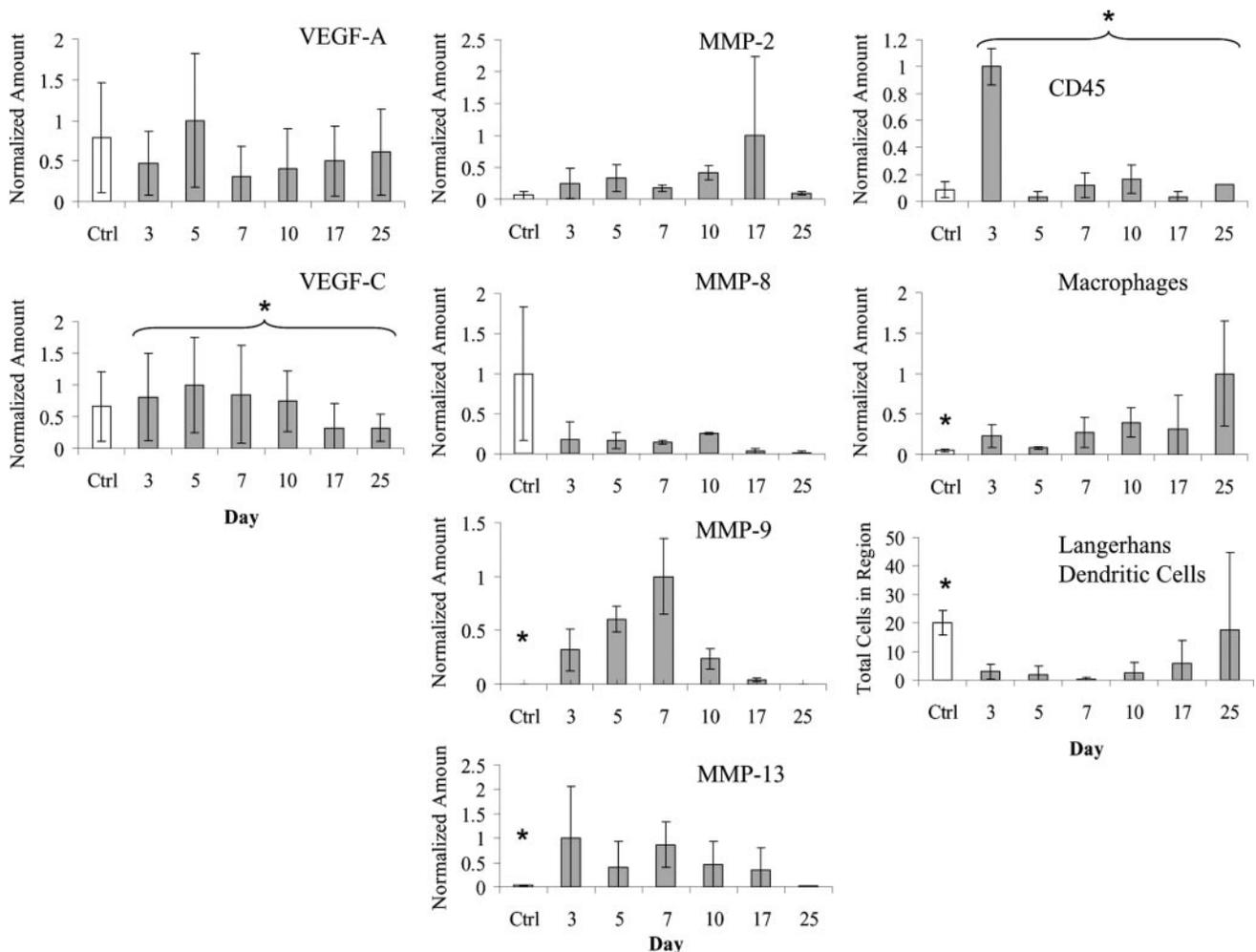

Fig. 4. Comparison of relative temporal expression patterns of VEGF-A and VEGF-C, matrix metalloproteinases (MMPs), and immune cells during regeneration. VEGF-A expression was highest at initiation of angiogenesis (*day 5*). VEGF-C expression was highest during initiation of lymphangiogenesis (*days 5–10*) and was reduced during organization phase (*day 17* and later). Expression of MMP-2 peaked during lymphangiogenesis. MMP-8 expression was very low throughout regeneration. MMP-9 was high at early times but decreased after *day 7*, whereas MMP-13 expression was highest before *day 10*, just preceding macrophage infiltration. Early infiltration of CD45^{+} immune cells at *day 3* primarily reflects neutrophils. Macrophages (F4/80^{+}) were highest after *day 10*, correlating with the onset of LEC infiltration. Langerhans dendritic cells (langerin[+]) did not repopulate region until *day 17* and later, when LECs were present and undergoing vessel organization. *$P < 0.05$ (over control indicates significant change in regeneration, and over bracket indicates temporal significance during regeneration).

(8, 36), endothelial cell migration (10, 11, 24), and vasculo-genesis (17, 24); we found that MMP-2 expression (Fig. 4) increased after *day 10*, concurrent with blood angiogenesis and at the initiation of lymphangiogenesis. Surprisingly, MMP-9 expression was very low after *day 7*, so its link to endothelial cell migration might be more important for blood angiogenesis but not critical to lymphangiogenesis. MMP-13 has been demonstrated to play a critical role in blood neovascularization (44) in conjunction with macrophages, which help induce angiogenic sprouting by using MMPs to extravasate from blood vessels (23). MMP-13 expression appeared to peak early, by *day 7*, thus preceding elevated macrophage numbers in the regenerating region (below). Although a role in blood neovascularization has been established (44), it is possible that MMP-13 activity is only critical for revascularization by mechanisms dependent on sprouting from the existing vasculature. MMP-8 expression was very low at all times in the regenerating tissue, despite other observations that it is upregulated in dermal wounds by neutrophils (25).

To examine the hypothesis that MMP-9 is not necessary for adult dermal lymphangiogenesis, we examined lymphatic regeneration in transgenic mice lacking MMP-9. The regenerating regions of these MMP-9-deficient mice were stained for LECs and BECs at *day 17* and *day 60*. There were no observable differences in the extent or morphology of either lymphatic or blood vessels in the regenerating region of these mice compared with matched wild-type control mice (Fig. 5*A*). Additionally, the number of LECs identified in the regenerating region at *day 17*, a critical time point in regeneration, was

the same between the MMP-deficient mice and matched wild-type controls ($P = 0.48$) (Fig. 5*B*). This is not inconsistent with other reports that showed minimal differences in blood angiogenesis in MMP-9-deficient mice (21, 27). It has been suggested that MMP-2 might have a more crucial role than MMP-9 in retinal angiogenesis (27) and that synergy between MMP-2 and -9 is essential for tumor vascularization (21); our data suggest that MMP-2 might be more important in lymphangiogenesis, at least in regenerating mouse skin, than MMP-9.

The temporal expression patterns of each of the MMPs surveyed correlated with the results of other wound healing studies (18, 19, 25, 30). Although it was not possible to define the exact role of each MMP due to its release by many cell types, including infiltrating immune cells, keratinocytes, and endothelial cells, as well as potentially overlapping and/or redundant roles in many different components of the skin regeneration process, our data demonstrate that, in terms of timing, MMP-2 was the most closely correlated to the onset of lymphangiogenesis and that lymphangiogenesis appeared normal in MMP-9 null mice.

Immune cell infiltration. Macrophages and dendritic cells, as antigen-presenting immune cells, utilize lymphatic vessels in adaptive immunity and may be involved in lymphangiogenesis (20); furthermore, macrophages both secrete VEGF-C (32) and chemotact up a VEGF-C gradient (35). We found that macrophage numbers were much higher during regeneration ($P = 0.001$) and peaked during LEC migration and organization at *days 17–25* ($P = 0.058$), hinting that macrophages may contribute to lymphangio-genesis as it does in blood angiogenesis (22) and consistent with recent findings that macrophages are necessary in inflammation-induced corneal lymphangiogenesis (20). Total immune cell numbers peaked at *day 3* ($P < 0.001$) (Fig. 4). These early infiltrating immune cells at *day 3* were typically neutrophils, as evidenced by polymorphonuclear Giemsa staining (data not shown). Very few Langerhans dendritic cells, normally present in the epidermis, were seen in the regenerating region until *day 17* or *25*, presumably when the regenerated epidermis is sufficiently integrated ($P = 0.028$). Because of intense immune cell infiltration during inflammation and in the wound healing response, exact roles for immune cells were difficult to discern; however, the correlation of macrophage infiltration with lymphangiogenesis at later times supports the prospective role of macrophages in lymphangiogenesis.

In conclusion, this study of lymphangiogenesis in regenerating skin provides new insight into adult lymphatic regeneration in a physiologically relevant environment and correlates potential contributing factors, such as MMPs and immune cells, to this process. We showed that migrating LECs populate the regenerating region in the direction of interstitial fluid flow and then grow together in a vasculogenesis-like fashion to form a new interconnected network of lymphatic vessels. Also, we demonstrated that interstitial flow is necessary for the organization of LECs into a functional network, whereas MMP-9 was not. Among the factors examined, the timing of MMP-2 and macrophages was more closely correlated to the late infiltration of LECs in the regenerating region, whereas basement membrane begins to develop only after the lymphatic structures have organized into functional vessels.
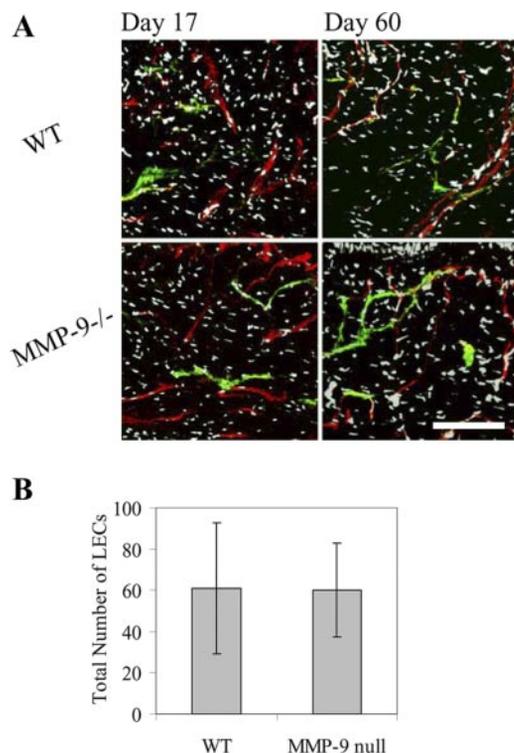

Fig. 5. No differences were seen in lymphatic regeneration in MMP-9 null (MMP-9$^{-/-}$) mice vs. matched wild-type (WT) controls. *A*: regenerated blood (red) and lymphatic (green) vessels in MMP-9 null mice were morphologically indistinguishable to those in control mice at *days 17* and *60*. Bar = 150 μm. *B*: number of LECs counted in regenerating region at *day 17* was not different between mouse strains ($P = 0.48$).

REFERENCES

1. **Achen MG, Jeltsch M, Kukk E, Makinen T, Vitali A, Wilks AF, Alitalo K, and Stacker SA.** Vascular endothelial growth factor D (VEGF-D) is a ligand for the tyrosine kinases VEGF receptor 2 (Flk1) and VEGF receptor 3 (Flt4). *Proc Natl Acad Sci USA* 95: 548–553, 1998.
2. **Achen MG, McColl BK, and Stacker SA.** Focus on lymphangiogenesis in tumor metastasis. *Cancer Cell* 7: 121–127, 2005.
3. **Balbin M, Fueyo A, Knauper V, Pendas AM, Lopez JM, Jimenez MG, Murphy G, and Lopez-Otin C.** Collagenase 2 (MMP-8) expression in murine tissue-remodeling processes analysis of its potential role in post-partum involution of the uterus. *J Biol Chem* 273: 23959–23968, 1998.
4. **Boardman KC and Swartz MA.** Interstitial flow as a guide for lymphangiogenesis. *Circ Res* 92: 801–808, 2003.
5. **Cao Y, Linden P, Farnebo J, Cao R, Eriksson A, Kumar V, Qi JH, Claesson-Welsh L, and Alitalo K.** Vascular endothelial growth factor C induces angiogenesis in vivo. *Proc Natl Acad Sci USA* 95: 14389–14394, 1998.
6. **Carmeliet P.** VEGF as a key mediator of angiogenesis in cancer. *Oncology* 69: 4–10, 2005.
7. **Gale NW, Thurston G, Hackett SF, Renard R, Wang Q, McClain J, Martin C, Witte C, Witte MH, Jackson D, Suri C, Campochiaro PA, Wiegand SJ, and Yancopoulos GD.** Angiopoietin-2 is required for postnatal angiogenesis and lymphatic patterning, and only the latter role is rescued by Angiopoietin-1. *Dev Cell* 3: 411–423, 2002.
8. **Gillard JA, Reed MW, Buttle D, Cross SS, and Brown NJ.** Matrix metalloproteinase activity and immunohistochemical profile of matrix metalloproteinase-2 and -9 and tissue inhibitor of metalloproteinase-1 during human dermal wound healing. *Wound Repair Regen* 12: 295–304, 2004.
9. **Goldman J, Le TX, Skobe M, and Swartz MA.** Overexpression of VEGF-C causes transient lymphatic hyperplasia but not increased lymphangiogenesis in regenerating skin. *Circ Res* 96: 1193–1199, 2005.
10. **Haas TL, Davis SJ, and Madri JA.** Three-dimensional type I collagen lattices induce coordinate expression of matrix metalloproteinases MT1-MMP and MMP-2 in microvascular endothelial cells. *J Biol Chem* 273: 3604–3610, 1998.
11. **Jadhav U, Chigurupati S, Lakka SS, and Mohanam S.** Inhibition of matrix metalloproteinase-9 reduces in vitro invasion and angiogenesis in human microvascular endothelial cells. *Int J Oncol* 25: 1407–1414, 2004.
12. **Jeltsch M, Kaipainen A, Joukov V, Meng X, Lakso M, Rauvala H, Swartz M, Fukumura D, Jain RK, and Alitalo K.** Hyperplasia of lymphatic vessels in VEGF-C transgenic mice. *Science* 276: 1423–1425, 1997.
13. **Jiang X and Couchman JR.** Perlecan and tumor angiogenesis. *J Histochem Cytochem* 51: 1393–1410, 2003.
14. **Joukov V, Pajusola K, Kaipainen A, Chilov D, Lahtinen I, Kukk E, Saksela O, Kalkkinen N, and Alitalo K.** A novel vascular endothelial growth factor, VEGF-C, is a ligand for the Flt4 (VEGFR-3) and KDR (VEGFR-2) receptor tyrosine kinases. *EMBO J* 15: 290–298, 1996.
15. **Kinsella MG, Tran PK, Weiser-Evans MC, Reidy M, Majack RA, and Wight TN.** Changes in perlecan expression during vascular injury: role in the inhibition of smooth muscle cell proliferation in the late lesion. *Arterioscler Thromb Vasc Biol* 23: 608–614, 2003.
16. **Kukk E, Lymboussaki A, Taira S, Kaipainen A, Jeltsch M, Joukov V, and Alitalo K.** VEGF-C receptor binding and pattern of expression with VEGFR-3 suggests a role in lymphatic vascular development. *Development* 122: 3829–3837, 1996.
17. **Lambert V, Wielockx B, Munaut C, Galopin C, Jost M, Itoh T, Werb Z, Baker A, Libert C, Krell HW, Foidart JM, Noel A, and Rakic JM.** MMP-2 and MMP-9 synergize in promoting choroidal neovascularization. *FASEB J* 17: 2290–2292, 2003.

18. **Lijnen HR, Lupu F, Moons L, Carmeliet P, Goulding D, and Collen D.** Temporal and topographic matrix metalloproteinase expression after vascular injury in mice. *Thromb Haemost* 81: 799–807, 1999.
19. **Madlener M, Parks WC, and Werner S.** Matrix metalloproteinases (MMPs) and their physiological inhibitors (TIMPs) are differentially expressed during excisional skin wound repair. *Exp Cell Res* 242: 201–210, 1998.
20. **Maruyama K, Ii M, Cursiefen C, Jackson DG, Keino H, Tomita M, Van Rooijen N, Takenaka H, D'Amore PA, Stein-Streilein J, Losordo DW, and Streilein JW.** Inflammation-induced lymphangiogenesis in the cornea arises from CD11b-positive macrophages. *J Clin Invest* 115: 2363–2372, 2005.
21. **Masson V, de la Ballina LR, Munaut C, Wielockx B, Jost M, Maillard C, Blacher S, Bajou K, Itoh T, Itohara S, Werb Z, Libert C, Foidart JM, and Noel A.** Contribution of host MMP-2 and MMP-9 to promote tumor vascularization and invasion of malignant keratinocytes. *FASEB J* 19: 234–236, 2005.
22. **Moldovan NI.** Role of monocytes and macrophages in adult angiogenesis: a light at the tunnel's end. *J Hematother Stem Cell Res* 11: 179–194, 2002.
23. **Moldovan NI, Goldschmidt-Clermont PJ, Parker-Thornburg J, Shapiro SD, and Kolattukudy PE.** Contribution of monocytes/macrophages to compensatory neovascularization. The drilling of metalloelastase-positive tunnels in ischemic myocardium. *Circ Res* 87: 378–384, 2000.
24. **Nakamura ES, Koizumi K, Kobayashi M, and Saiki I.** Inhibition of lymphangiogenesis-related properties of murine lymphatic endothelial cells and lymph node metastasis of lung cancer by the matrix metalloproteinase inhibitor MMI270. *Cancer Sci* 95: 25–31, 2004.
25. **Nwomeh BC, Liang HX, Cohen IK, and Yager DR.** MMP-8 is the predominant collagenase in healing wounds and nonhealing ulcers. *J Surg Res* 81: 189–195, 1999.
26. **Oh SJ, Jeltsch MM, Birkenhager R, McCarthy JE, Weich HA, Christ B, Alitalo K, and Wilting J.** VEGF and VEGF-C: specific induction of angiogenesis and lymphangiogenesis in the differentiated avian chorioallantoic membrane. *Dev Biol* 188: 96–109, 1997.
27. **Ohno-Matsui K, Uetama T, Yoshida T, Hayano M, Itoh T, Morita I, and Mochizuki M.** Reduced retinal angiogenesis in MMP-2-deficient mice. *Invest Ophthalmol Vis Sci* 44: 5370–5375, 2003.
28. **Oliver G and Alitalo K.** The lymphatic vasculature: recent progress and paradigms. *Annu Rev Cell Dev Biol* 21: 457–483, 2005.
29. **Pytowski B, Goldman J, Persaud K, Wu Y, Witte L, Hicklin DJ, Skobe M, Boardman KC, and Swartz MA.** Complete and specific inhibition of adult lymphatic regeneration by a novel VEGFR-3 neutralizing antibody. *J Natl Cancer Inst* 97: 14–21, 2005.
30. **Salo T, Makela M, Kylmaniemi M, Autio-Harmainen H, and Larjava H.** Expression of matrix metalloproteinase-2 and -9 during early human wound healing. *Lab Invest* 70: 176–182, 1994.
31. **Schacht V, Ramirez MI, Hong YK, Hirakawa S, Feng D, Harvey N, Williams M, Dvorak AM, Dvorak HF, Oliver G, and Detmar M.** T1alpha/podoplanin deficiency disrupts normal lymphatic vasculature formation and causes lymphedema. *EMBO J* 22: 3546–3556, 2003.
32. **Schoppmann SF, Birner P, Stockl J, Kalt R, Ullrich R, Caucig C, Kriehuber E, Nagy K, Alitalo K, and Kerjaschki D.** Tumor-associated macrophages express lymphatic endothelial growth factors and are related to peritumoral lymphangiogenesis. *Am J Pathol* 161: 947–956, 2002.
33. **Segev A, Nili N, and Strauss BH.** The role of perlecan in arterial injury and angiogenesis. *Cardiovasc Res* 63: 603–610, 2004.
34. **Sephel GC, Kennedy R, and Kudravi S.** Expression of capillary basement membrane components during sequential phases of wound angiogenesis. *Matrix Biol* 15: 263–279, 1996.
35. **Skobe M, Hamberg LM, Hawighorst T, Schirner M, Wolf GL, Alitalo K, and Detmar M.** Concurrent induction of lymphangiogenesis, angiogenesis, and macrophage recruitment by vascular endothelial growth factor-C in melanoma. *Am J Pathol* 159: 893–903, 2001.
36. **Stamenkovic I.** Extracellular matrix remodelling: the role of matrix metalloproteinases. *J Pathol* 200: 448–464, 2003.
37. **Swartz MA.** The physiology of the lymphatic system. *Adv Drug Delivery Res* 50: 3–20, 2001.
38. **Swartz MA, Berk DA, and Jain RK.** Transport in lymphatic capillaries. I. Macroscopic measurements using residence time distribution theory. *Am J Physiol Heart Circ Physiol* 270: H324–H329, 1996.

39. **Swartz MA and Boardman KC Jr.** The role of interstitial stress in lymphatic function and lymphangiogenesis. *Ann NY Acad Sci* 979: 197–210, 2002.

40. **Tammela T, Saaristo A, Lohela M, Morisada T, Tornberg J, Norrmen C, Oike Y, Pajusola K, Thurston G, Suda T, Yla-Herttuala S, and Alitalo K.** Angiopoietin-1 promotes lymphatic sprouting and hyperplasia. *Blood* 105: 4642–4648, 2005.

41. **Whitelock JM, Graham LD, Melrose J, Murdoch AD, Iozzo RV, and Underwood PA.** Human perlecan immunopurified from different endothelial cell sources has different adhesive properties for vascular cells. *Matrix Biol* 18: 163–178, 1999.

42. **Wigle JT and Oliver G.** Prox1 function is required for the development of the murine lymphatic system. *Cell* 98: 769–778, 1999.

43. **Yuan L, Moyon D, Pardanaud L, Breant C, Karkkainen MJ, Alitalo K, and Eichmann A.** Abnormal lymphatic vessel development in neuropilin 2 mutant mice. *Development* 129: 4797–4806, 2002.

44. **Zijlstra A, Aimes RT, Zhu D, Regazzoni K, Kupriyanova T, Seandel M, Deryugina EI, and Quigley JP.** Collagenolysis-dependent angiogenesis mediated by matrix metalloproteinase-13 (collagenase-3). *J Biol Chem* 279: 27633–27645, 2004.